X-ray studies of the hexatic phase in liquid crystals with a crystal-*B* – hexatic-*B* – smectic-*A* phase sequence

Ewa Górecka,[1,2,3] Li Chen,[1] Wiesław Pyżuk,[3] Adam Krówczyński,[3] and Satyendra Kumar[1,2]
[1]*Liquid Crystal Institute, Kent State University, Kent, Ohio 44242*
[2]*Department of Physics, Kent State University, Kent, Ohio 44242*
[3]*Department of Chemistry, University of Warsaw, 02-089 Warszawa, Al. Żwirki i Wigury 101, Poland*
(Received 3 June 1994)

Free-standing monodomain thick films of three liquid crystalline compounds were examined by x-ray scattering. These compounds exhibit a unique enantiotropic crystal-*B*–hexatic-*B*–smectic-*A* phase sequence with no evidence of herringbone order. The hexatic order parameter C_6 changes in the hexatic phase with critical exponent $\beta=0.15\pm0.03$. Temperature dependence of the in-plane positional order correlation length suggests a strongly first-order hexatic-*B* to crystal-*B* phase transition with indiscernible enthalpy change.

PACS number(s): 64.70.Md, 61.30.Gd

Nearly 15 years ago, it was realized that the phase transition between a two-dimensional (2D) crystal and a liquid phase can occur through an intermediate *hexatic* phase [1]. In the *hexatic* phase, positional order is short range but bond orientational order (BOO) persists over quasi-long-range [2]. Although few examples of BOO systems have been found in nature, it seems that only liquid crystals (LC's) are relatively rich in hexatic phases [3]. Tilted hexatic phases, smectic-*I* and -*F*, are common among calamitic mesogens, but untilted hexatic smectic-*B* (Hex-*B*) phase was encountered only in a few substances [3]. It is very rare to find mesogens with the phase sequence: crystal-*B* (Cry-*B*)–Hex-*B*–smectic-*A* (Sm-*A*). Here, the Hex-*B* phase is an intermediate phase between a crystal and a liquidlike Sm-*A* phase [4].

The fluid to hexatic phase transition in liquid crystals is described by a hexatic order parameter, $\Psi_6(\mathbf{x})=e^{i6\theta(\mathbf{r})}$, dependent on the spatial orientation $\theta(\mathbf{r})$ of the local crystallographic axes. This complex, two-component order parameter suggests that the transition should belong to the *XY* universality class. For three-dimensional (3D) systems in this universality class, the order parameter and specific heat critical exponents [5] β and α are expected to be 0.35 and -0.007, respectively. Since the previous heat capacity measurements yielded α close to a tricritical value of 0.5, the existence of a tricritical point on the phase transition line was postulated [3]. The coupling between the hexatic order and one or more of the other orders is believed to be responsible for the presence of the tricritical point. For example, in the most extensively studied compounds of *n*-alkyl-4′-*n*-alkoxybiphenyl-4-carboxylate (*nm*OBC) series, fluctuations of in-plane herringbone order (HBO) were assumed to exist [9] and confirmed by x-ray measurements in 75OBC [6] and in 65OBC [7] compounds. Also, fluctuations of in-plane crystal density [10] and smectic layers [11] were considered responsible for the presence of the tricritical point. To experimentally test the validity of these ideas, it is essential to select appropriate LC materials which differ in the extent of these orders. In particular, a study of materials which do not exhibit herringbone arrangement of molecules in the hexatic and crystal phases could prove very useful.

Recently, several homologous series of enaminoketone compounds have been synthesized in which this unique phase sequence is observed [4]. These compounds exhibit the Cry-*B* phase below the Hex-*B*, rather than the commonly encountered [3,12] and highly ordered crystalline-*E* phase. In contrast to *nm*OBC compounds, there is no x-ray evidence of HBO in the Hex-*B* and Cry-*B* phases of these compounds, indicating that the coupling between BOO and HBO is absent. Furthermore, these are the only known materials which permit the study of both phase transitions in a single system. Three compounds [8] were selected for their convenient phase transition temperatures as well as appropriate temperature ranges of the hexatic phase (11.2 K, 9.0 K, and 5.0 K for RFL6, FLU9, and PIR5, respectively). RFL*n* and FLU*n* homologous series have similar phase diagrams, with three transition lines meeting at the Cry-*B*–Hex-*B*–Sm-*A* triple point [10].

In this paper, we report results of our x-ray scattering study of the Cry-*B*–Hex-*B* and Hex-*B*–Sm-*A* phase transitions. High-resolution x-ray scattering technique augmented by low-resolution measurements was used to study both positional and bond orientational order in RFL6 [8]. The lack of HBO makes these materials ideal for the study of true hexatic phases and the results presented here shed new light on the nature of hexatic systems.

Unlike the tilted hexatic smectic-*I* and -*F* phases, in which single-domain samples, crucial for quantitative study, can be easily obtained with the use of an external magnetic field owing to its coupling to molecular tilt, aligned samples are very difficult to obtain for the Hex-*B* phase [6,13]. However, for our materials, surface and interplanar forces were sufficient to produce well aligned, thick (>10 μm) free-standing films. These films were found to be stable for several weeks. For two of the three compounds studied, RFL6 and PIR5, we succeeded in obtaining perfectly aligned films. Their monodomain structure was confirmed by examining wide angle x-ray

scattering patterns obtained with Siemens X-1000 area detector. The patterns remained well defined and unchanged when different areas of the film were illuminated with x-ray beam of 0.5 mm diameter. The in-plane reflections exhibited an almost perfect six-fold symmetry (Fig. 1), which pointed to strong orientational interlayer correlations making the hexatic phase a three dimensional phase [6].

High-resolution x-ray experiments were performed using 18-kW Rigaku rotating anode generator, a pair of Ge(111) single crystals used as monochromator and analyzer, and a four-circle Huber goniometer. The resulting longitudinal and in-plane transverse (resolutions) full width at half maximum (FWHM) were $\Delta q_{\parallel}=4\times10^{-4}$ Å^{-1} and $\Delta q_{\perp}=2\times10^{-5}$ Å^{-1}, respectively. The samples were placed in an oven with thermal stability of better than ±20 mK. Details of the experimental setup can be found in Ref. [14]. Longitudinal ($q_{\parallel}$-) scans were carried out to determine the in-plane correlation length $\xi_{\parallel}$. The data were fitted to a generalized Lorentzian line shape; $S(q_{\parallel})\sim[1+\xi_{\parallel}^2(q_{\parallel}-q_0)^2]^{-a}$ with an adjustable exponent a. At all temperatures, the best fit value of a was close to unity. Representative fits are shown in Fig. 2 and the temperature dependence of $\xi_{\parallel}$ in Fig. 3. Evidently the correlation length gradually increased with decreasing temperature for the compounds examined and showed no signs of the critical behavior at the Hex-*B*–Cry-*B* transition. Clear deviations from linearity of $\xi_{\parallel}$ vs T were found only for PIR5, where $\xi_{\parallel}$ increases from 85 to 125 Å. The maximum value of $\xi_{\parallel}$ near this phase transition, 225±5 Å, was obtained for FLU9. This value, when compared with much larger values of more than 5000 Å in the Cry-*B* phase very close to the transition, points to a strongly discontinuous character of Hex-*B*–Cry-*B* phase transition. For FLU9, we were even able to observe the coexistence of the Hex-*B* and Cry-*B* phases for a narrow (<0.1 K) temperature range [Fig. 2(c)].

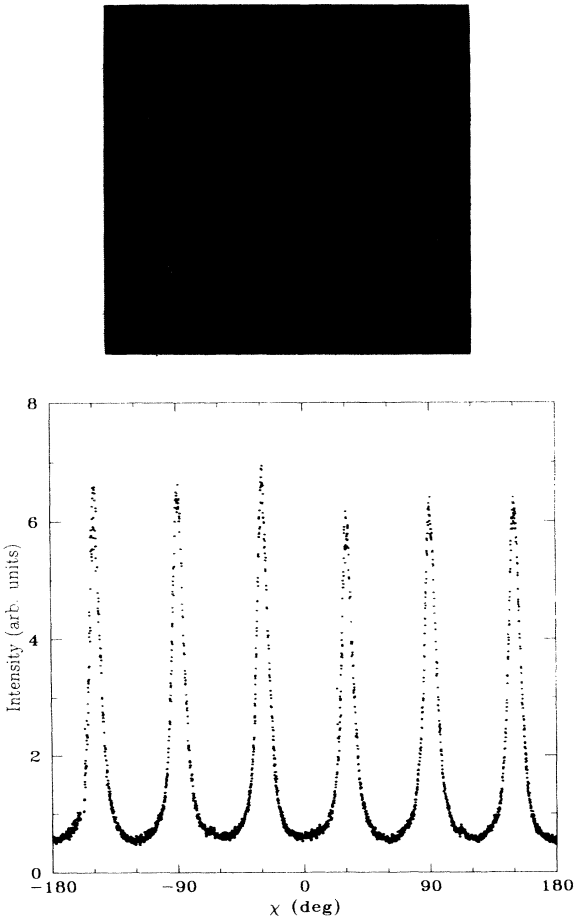

FIG. 1. X-ray diffraction pattern for 0.1 mm thick RFL6 sample 1.5 K below the Sm-*A*–Hex-*B* phase transition and the corresponding χ scan.

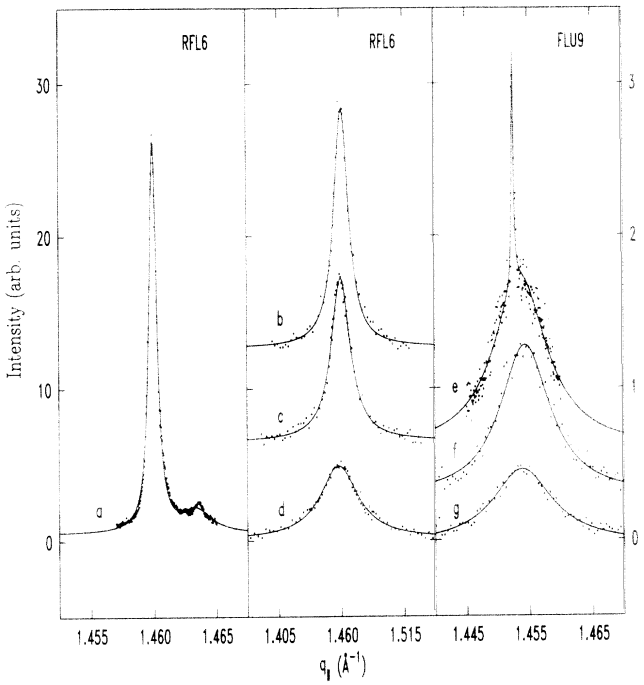

FIG. 2. $q_{\parallel}$-scans for RFL6 in Cry-*B* phase (a), and in Hex-*B* phase (b)–(d) along with the best fits to a single Lorentzian or a sum of two Lorentzians (for two phase coexistence shown in (e). The scans for FLU9 in Hex-*B*–Cry-*B* coexistence region (e) and in pure Hex-*B* phase (f)–(g). Distances from the Hex-*B*–Cry-*B* transition and the corresponding values of $\xi_{\parallel}$ are (a) −0.04 K, >5000 Å, i.e., resolution limited, (b) 0.12 K, 133 Å, (c) 2.22 K, 101 Å, (d) 645 K, 50 Å, (f) 0.25 K, 217 Å, (g) 1.1 K, 179 Å. Small peak in (a) is due to $K_{\alpha 2}$.

The first-order Hex-*B*–Cry-*B* phase transition, expected on the basis of symmetry arguments [10], was confirmed by a strong discontinuity in $\xi_{\parallel}$ in spite of relatively small transition enthalpy. In differential scanning calorimetry (DSC) thermograms, a sharp peak for PIR5 and a much less pronounced peak for RFL6 were observed ($\Delta H=0.51$ and 0.02 ± 0.005 J g^{-1}, respectively), pointing to a weakly first-order transition. There was no detectable peak ($\Delta H<0.005$ J g^{-1}) at this transition for FLU9, suggesting an almost-continuous phase transition. Furthermore, for all homologous series of hexatic enaminoketones, the transition enthalpy rapidly decreased

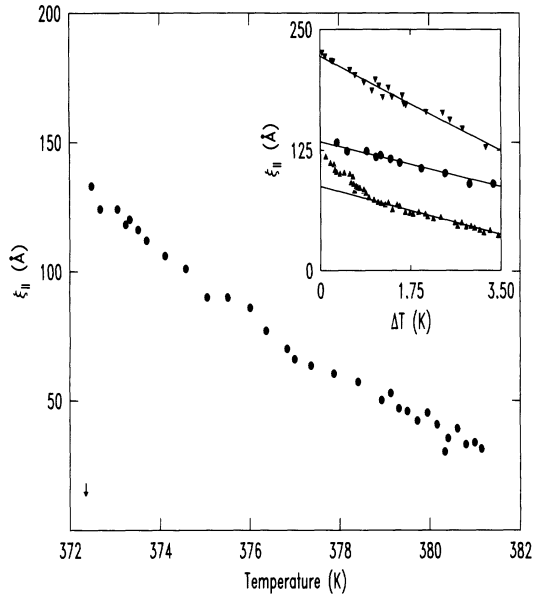

FIG. 3. Temperature dependence of the in-plane positional order correlation length $\xi_{\|}$ for RFL6. The line is drawn as a guide to the eye. The arrow near 372.5 K denotes the low-temperature limit of the Hex-*B* phase. Data close to Cry-*B*–Hex-*B* phase transition for RFL6, FLU9, and PIR5 are compared in the inset.

along the Cry-*B*–Hex-*B* phase transition line and vanished at an apparent critical point [4] even though the transition remained discontinuous. Evidently the relation between thermal effects accompanying phase transitions and changes in the structure of involved phases deserves careful consideration. On the basis of our results, we can exclude the changes in the in-plane or interlayer positional correlation length as the main factor responsible for the phase transition enthalpy. Further, we found the discontinuities in the in-plane and interlayer molecular distances to be very small, less than 0.3×10^{-2} Å and 1.5×10^{-2} Å, respectively, at the Cry-*B*–Hex-*B* phase transition in FLU9 and PIR5. In contrast, at the Hex-*B*–Sm-*A* phase transition where the thermal effects are pronounced [3,4], much larger changes in the in-plane intermolecular distance were observed [6]. Therefore it is possible that the relevant thermal effects arise mostly from the changes in the in-plane density. It is interesting to note that the extent of the in-plane positional correlation length plays a key role in the formation of hexatic monodomains. For instance, materials with small $\xi_{\|}$ were found to easily form monodomains (case of PIR5) while materials that were "more crystalline," i.e., possessed large $\xi_{\|}$ (such as FLU9), did not form well-aligned films.

It is clear from Fig. 3 that $\xi_{\|}$ decreases to a value of ca. 25 Å at 2 K above the transition to the Sm-*A* phase, which is close to the value typically obtained in fluid smectics. Although we were not able to determine precisely behavior of $\xi_{\|}$ close to Hex-*B*–Sm-*A* transition, due to low scattering intensity, small values of $\xi_{\|}$ suggests that transition cannot be strongly first order. This conclusion was also supported by our low-resolution x-ray measurements, which allowed us to determine the temperature evolution of $6n$-fold order parameters $C_{6n}=\mathrm{Re}\langle\Psi_0^n\rangle$. These parameters were evaluated from the analysis of scattering profiles (Fig. 1) by fitting the χ-scans (Fig. 4) to a Fourier cosine series [15].

$$S(\chi)=I_0[\tfrac{1}{2}+\sum_n C_{6n}\cos 6n(\chi-\chi_0)]+I_{\mathrm{bc}}\ .$$

Here χ_0 is a reference χ angle and I_{bc} is the background intensity. The number of necessary parameter C_{6n} in data analysis depends on the magnitude of the basic order parameter C_6. Due to the scaling relations between them (see below), the number of harmonics that remain significant decreases with decreasing value of C_6. For example, far from the phase transition $n<25$, and close to the transition, values of $n<10$ were found sufficient to give good fits. No substantial differences were noticed between fits for free order parameters and for parameters scaled as $C_{6n}=C_0^{\sigma_n}$, where [10] $\sigma_n=n+\lambda n(n-1)$. This scaling relation, previously found to hold for tilted hexatic phases, also works well for the Hex-*B* phase. However, we had to keep λ as an adjustable parameter. To take into account the slight differences ($<3\%$) in the amplitudes of χ peaks, each peak was fitted individually and best fit parameters, obtained for the six peaks, averaged. Differences between the values of C_{6n} were less than 5%.

The resulting correction parameter λ and hexatic order parameter C_6 are shown in Fig. 5. Deep in the Hex-*B* phase, λ is close to zero which means the mean-field approximation works well in this temperature range. Its value increases significantly to ca. 0.2, near the *A* phase, where $C_6\to0$. Since the 3D *XY* value of $\lambda=0.295$ was

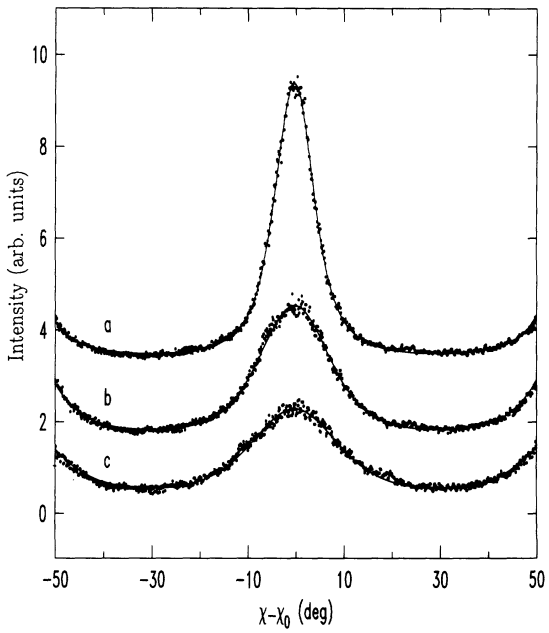

FIG. 4. χ-scans and fits to the function $S(\chi)$ at selected temperatures in the Hex-*B* phase. The distance from the Hex-*B*–Sm-*A* transition are (a) 2.77 K, (b) 0.45 K, and (c) 0.10 K. The curves have been shifted vertically for clarity.

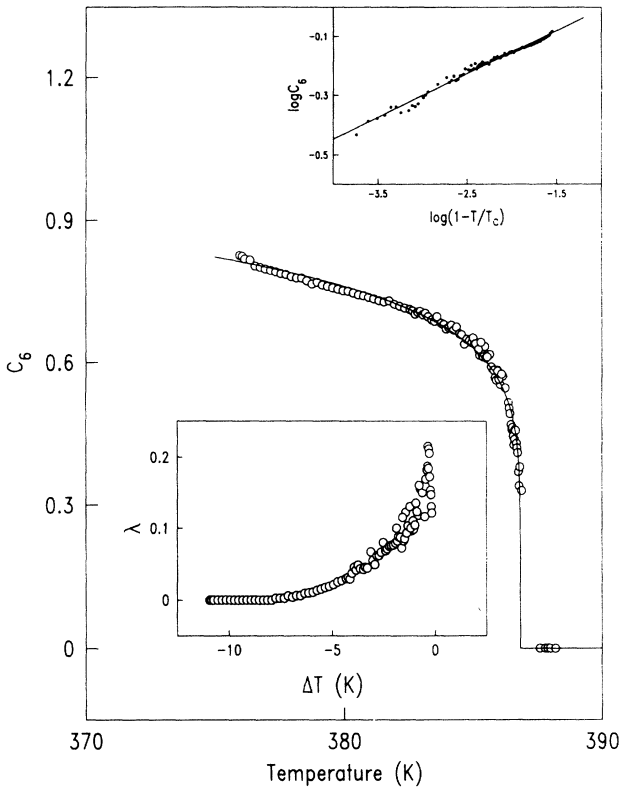

FIG. 5. Bond orientational parameter C_6 vs temperature for RFL6 and the power-law fit with exponent 0.15. The lower inset shows the coefficient λ. The upper inset shows a $\log_{10}$-$\log_{10}$ plot of C_6 vs reduced temperature.

not reached, the RFL6 system did not appear to fully cross over from the mean field to the *XY* regime. It would be desirable to check whether *XY* behavior is exhibited in the two-dimensional (2D) limit as an exact 2D *XY* value of $\lambda=1$ has been reported [16] for superthin films Hex-*B* samples. The temperature dependence of C_6 is well described by a power law and exhibits no pretransitional increase in the Sm-*A* phase. The critical exponent β is found to be 0.15 ± 0.03. In these fits, the transition temperature was treated as an adjustable parameter and its best fit value corresponded well with the temperature at which the modulation in χ-scans disappeared. However, our C_6 data were not sufficiently accurate to confirm the continuity of the phase transitions. The value obtained for β is comparable to the value for another orthogonal system. For example, $\beta=0.19\pm0.03$ for 65 OBC was previously indirectly estimated from pretransitional birefringence [17], and it is in agreement with the prediction for the three-state Potts model in three dimensions [3]. However, because of the low value of λ and lack of HBO, and hence three-state Potts symmetry, proximity of a tricritical point is likely for RFL6. A strong signature of *XY*-like fluctuations is the increase in λ in the vicinity of the Hex-*B*–Sm-*A* phase transition as observed for TB6A [18] near the smectic-*F* to -*C* phase transition. Most probably, the similarity between untilted phases of RFL6 and tilted phases of TB6A results from their near-tricritical behavior as well as a weak coupling between BOO and the tilt field in the latter compound.

In conclusion, our results show that there are no significant differences in hexatic properties between systems with and without herringbone order. Our value of the exponent of the hexatic order parameter in RFL6 is consistent with the heat capacity exponents reported for several hexatic system with HBO [3]. Thus the HBO cannot be the factor responsible for the discrepancy between experimental results and expectations of 3D *XY* like behavior. Further, we found that the changes in the degree of the positional order are not related to the thermal effects at the hexatic-crystal phase transition which suggest a strong first-order nature in spite of no measurable transition enthalpy.

Fulbright Foundation's support of E.G.'s visit to Kent State University is gratefully acknowledged. This work was supported in part by Polish Ministry of National Education (Grant No. UW/502-BST-29/93) and by NSF Science and Technology Center ALCOM Grant No. NSF-DMR-89-20147.

[1] B. I. Halperin and D. R. Nelson, Phys. Rev. Lett. **41**, 121 (1978).

[2] J. D. Brock, in *Bond-Orientational Order in Condensed Matter Systems,* edited by K. J. Strandburg (Springer-Verlag, New York, 1992).

[3] C. C. Huang, in Ref. [2].

[4] W. Pyżuk, A. Krówczyński, and E. Górecka, Mol. Cryst. Liq. Cryst. **237**, 75 (1993); W. Pyżuk, E. Górecka, and A. Krówczyński, Liq. Cryst. **10**, 593 (1991).

[5] J. C. LeGuillon and J. Zinn-Justin, Phys. Rev. B **21**, 3976 (1980).

[6] R. Pindak, D. E. Moncton, S. D. Davey, and J. W. Goodby, Phys. Rev. Lett. **46**, 1135 (1981).

[7] C. C. Huang, R. Pindak, and G. Srajer, (1990) unpublished, cited according to C. C. Huang and T. Stoebe, Adv. Phys. **42**, 343 (1993).

[8] PIR5 stands for 1-(4′-pentyloxyphenylamino)-3[5″-(2″-methylpirydil)]-1propen-3-on; FLU9 for 1-(4′-nonyloxyphenylamino)-3-(4″-fluorophenyl)-1-propen-3-on; and RFL6 for 1-(4′-fluorphenylamino)-3(4″-hexylohyphenyl)-1-propen-3-on.

[9] R. Bruinsma and G. Aeppli, Phys. Rev. Lett. **48**, 1625 (1982).

[10] A. Aharony, R. J. Birgeneau, J. D. Brock, and J. D. Litster, Phys. Rev. Lett. **57**, 1012 (1986).

[11] J. D. Selinger, J. Phys. (Paris) **49**, 1387 (1988).

[12] T. Pitchford, G. Nounesis, D. Dumrongrattana, J. M. Viner, C. C. Huang, and J. W. Goodby, Phys. Rev. A **33**, 1938 (1985).

[13] S. C. Davey, J. Budai, J. W. Goodby, R. Pindak, and D. E. Moncton, Phys. Rev. Lett. **53**, 2129 (1984).

[14] P. Patel, Li Chen, and S. Kumar, Phys. Rev. E **47**, 2643

(1993).
[15] J. D. Brock, A. Aharony, R. J. Birgeneau, K. V. Evans-Lutterodt, J. D. Litster, P. M. Horn, G. B. Stevenson, and A. R. Tajbakhash, Phys. Rev. Lett. **57**, 98 (1986).
[16] M. Cheng, J. T. Ho, S. W. Hui, and R. Pindak, Phys. Rev. Lett. **61**, 550 (1988).
[17] C. Rosenblatt and J. T. Ho, Phys. Rev. A **26**, 2293 (1982).
[18] D. Y. Noh, J. D. Brock, J. D. Litster, R. J. Birgeneau, and J. W. Goodby, Phys. Rev. B **40**, 4920 (1989).

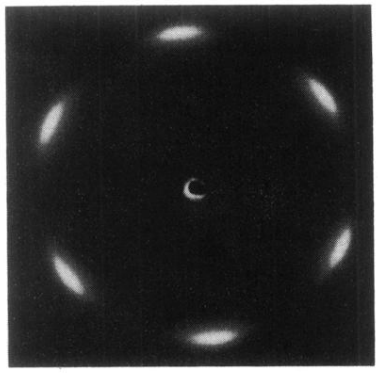

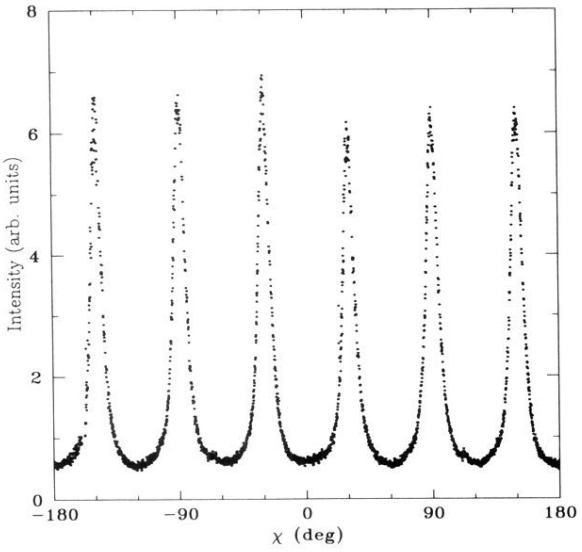

FIG. 1. X-ray diffraction pattern for 0.1 mm thick RFL6 sample 1.5 K below the Sm-*A*–Hex-*B* phase transition and the corresponding χ scan.